

Research on the Lightweight Drive Axle Housing of Electric Farm Management Machine

Tong ZHANG*, **, Huajun WANG***, Qiang YANG****

*College of Geophysics, Chengdu University of Technology, Chengdu, Sichuan 610059, China

**College of Mechanical and Electrical Engineering, Yibin University, Yibin, Sichuan 644000, China

***College of Geophysics, Chengdu University of Technology, Chengdu, Sichuan 610059, China,

E-mail: wanghuajun@cdu.edu.cn (Corresponding author)

****Science and Technology Department, Yibin University, Yibin, Sichuan 644000, China, E-mail:

scyqiang@163.com (Corresponding author)

<https://doi.org/10.5755/j02.mech.37764>

1. Introduction

The popularity of electric farm management machines helps to improve the living standards of rural residents, reduce transportation costs in rural areas, and improve economic benefits [1, 2]. It is one of the important directions of the development of new energy vehicles, which realizes the reduction of the overall weight of the vehicle by optimizing the structural design. This will not only improve the energy efficiency and range of electric vehicles but also improve the vehicle's power performance and handling while reducing the impact on the environment. Lightweight design not only helps to improve the endurance and performance of electric vehicles but also reduces production costs and enhances market competitiveness [3-6].

For the realization of the goal of vehicle lightweight, we can start with the lightweight chassis part. As a crucial part of the entire chassis structure - the drive axle, we can consider adjusting the dimensions of the axle housing, drilling holes in the non-bearing part or changing its material properties, processing technology and other methods to optimize the axle housing under the premise of ensuring the stiffness, strength and fatigue life of the drive axle housing. Reducing the vibration and noise of the axle housing during driving can achieve the effect of improving stiffness, strength, and service life, which are all important methods to improve the performance of the vehicle and reduce the weight [7-14].

Kurniawan et al. [15] chose the Mitsubishi L300 drive axle housing as the research object, and first conducted a detailed analysis of the load conditions in the fracture area of the axle housing. Then, they imported the three-dimensional model of the axle housing into the finite element analysis software and performed stress analysis. Through this process, they determined the location of the maximum Von Mises, the maximum shear stress, and the maximum principal stress in the axle housing. The regions with the largest stress values are very close to the locations where the actual fracture occurs, thus verifying the accuracy of the finite element analysis results and the consistency of the reality. Ognevskii et al. [16] conducted an in-depth study on the axle housing of the drive axle of heavy vehicles. They conducted experiments using electrothermal treatment technology and found that there was a significant correlation between the treatment temperature of the axle housing and its performance parameters such as stiffness. This experi-

mental study provides important reference data for finite element analysis of drive axle housing and promotes the application of the finite element method in this field. Fu et al. [17] used finite element analysis technology to conduct an in-depth study on the strength and stiffness of the axle housing. They cleverly designed the graded bushing in the stress concentration area of the axle housing, effectively reducing the local stress. This study not only improves the performance of the axle housing but also provides valuable reference information for the subsequent automotive design optimization work. Xu et al. [18] conducted an in-depth study on the differential housing made of ductile iron. Despite a series of experiments and improvement measures, they found that the weight of the shell was still too large to reduce. Then, they used the finite element method to change the housing material to aluminum alloy and compared the performance of the differential housing before and after the improvement in terms of strength and mode. The results show that the weight of the differential housing using aluminum alloy material is reduced by 60%, which opens up a new direction for the lightweight design of automobiles. Rishi et al. [19] focused on the production process of axle housing. Through technological innovation, they have successfully reduced material handling time, providing valuable experience for the axle housing production plant to improve production efficiency. Kumar et al. [20] have made new progress in the optimization design of axle housing. The optimized axle housing has a significant increase in fatigue life and a decrease in maximum stress concentration in the experiment that could affect the results.

Carry out experimental research based on the theoretical framework of the drive axle, comprehensively use static characteristics, modal characteristics analysis, fatigue life assessment, and other technical means to deeply study the axle housing and its components, and then guide product design based on the obtained analysis data, identify the defects in the product and the causes that may lead to the failure of the axle housing, ensure the reliability of the product, and provide theoretical basis. Make the drive axle have better technology, better parts-related design ideas, and finally improve the reliability of auto parts [21, 22]. In summary, the lightweight design with size optimization can effectively carry out the design of the drive axle housing.

The results show that the drive axle housing with lightweight design has good performance. The main contributions of this paper are as follows:

- Establish the three-dimensional model of the electric drive axle housing, import the model into the finite element, set the material parameters, and generate the finite element model.

- The force analysis of the drive axle housing under the maximum vertical force condition is proposed. The first 6 natural frequencies and modes were extracted.

- Through the analysis of the stress and deformation cloud map of the axle housing, the size of the axle housing part with the maximum stress and deformation is taken as the design variable, and the mass of the axle housing is taken as the response, correlation analysis is conducted to find out the parameters that have a greater impact on the quality as the design variable, and the Latin hypercube experimental design method, Kriging approximation model and multi-objective optimization algorithm are combined. Lightweight design with optimized dimensions for the axle housing.

2. Establishment of Finite Element Model of Drive Axle Housing

The first condition to ensure the success of finite element analysis is to build a high-quality finite element model. However, in order to reduce the computational effort and improve the computational efficiency, the micro-structural features that affect the meshing quality and the finite element analysis results are ignored without affecting the key parameters of the model.

The main parameters of the car and the drive axle housing are shown in Table 1 below.

The simplified two-dimensional model of the axle housing is shown in Fig. 1

2.1. 3D modeling process

1. Observe the two-dimensional engineering drawing to get the specific size of the axle housing, and imagine the approximate model effect drawing.

2. Select the reference surface of the upper view for sketch drawing: After entering the drawing module, draw the approximate shape of the model with curves and straight lines in the sketch, and apply dimensional and geometric constraints on it.

3. Stretch the sketch, rotate the boss, and then cut the excess part to get the rough model of the drive axle housing.

4. Then refine the model, using commands such as shell extraction, hole drilling, and mirror array.

Fig. 2 shows the simplified concrete model.

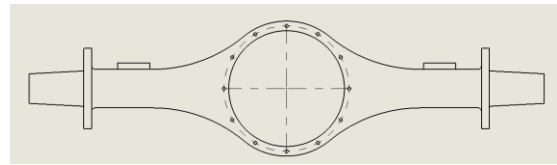


Fig. 1 Two-dimensional model of the axle housing

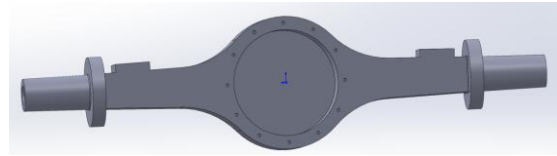


Fig. 2 3D model of drive axle housing

2.2. Finite element model establishment

1. Model import

Build a 3D model in SolidWorks, then click the file in the upper left corner to save as, in the save as dialog box to adjust the format to Parasolid (*.x_t; *.x_b), and then click Save.

2. Selection of materials

The material of the drive axle housing is cast steel material, and the specific material properties are shown in Table 2.

Create a new material and rename it ZG45 with input material density of 7850 kg/m^3 , Young's modulus set to $2.11 \times 10^{11} \text{ Pa}$, Poisson's ratio modified to 0.34, return to project analysis.

3. Meshing

The hexahedral mesh partition with higher calculation accuracy is selected. The generated grid model has 2075334 nodes, 1473920 cells, and the cell size is 5 mm.

4. Mesh quality

Click the metric in the grid properties interface to display, and then select grid quality to get ICONS, as shown in Fig. 3 respectively.

Through the analysis of the figures, it can be concluded that the use of 5 mm grid division is more reasonable, and the grid quality reaches 0.88.

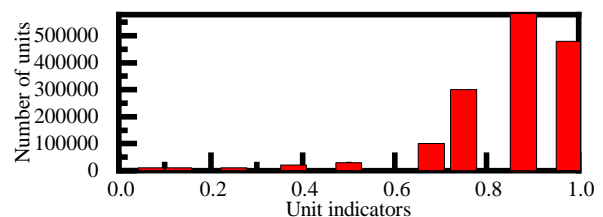


Fig. 3 Grid quality diagram of axle housing

Table 1

Main parameters of vehicle and drive axle housing

Total mass	4.495 t	Total length of axle housing	1603 mm
Rear track	1606 mm	Axle housing thickness	140 mm
Maximum torque	235 N · m	Pitch of leaf spring	853 mm
Maximum power	69.09 kW	Plate spring seat thickness	20 mm

3. Static and Dynamic Characteristics Analysis of Drive Axle Housing

The working environment and force of the drive

axle housing are complex and changeable conditions. Therefore, we will simplify the complex and changeable typical working conditions and carry out Von Mises analy-

sis, total deformation analysis, and constraint mode analysis, so as to provide a favorable reference for the subsequent lightweight research of the axle housing when it meets the requirements of parameters.

3.1. Drive axle housing force analysis

Under the maximum vertical force condition, we set the car in full load state, at this time, the car driving on the uneven road will be subjected to an impact load from the road surface. In the actual analysis, we should consider the situation in the ideal state, that is, only consider the impact load in the vertical direction of the force generated on the spring seat on both sides of the axle housing, ignoring the influence of other directions. We assume that the vertical load at this time is F_1 , and according to the force analysis diagram shown in Fig. 4, the stress state of the axle housing under the maximum vertical force condition is systematically discussed and analyzed.

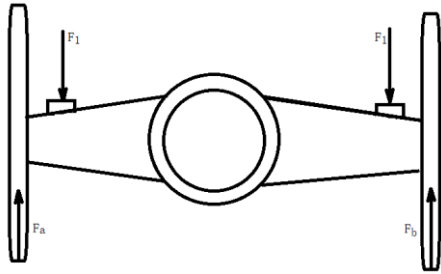


Fig. 4 Force analysis diagram under maximum vertical force condition

As shown in Fig. 4, the force on the axle housing spring plate at this time is as follows:

$$F_1 = F_a \times \delta = \frac{G_1}{2} \times \delta = \frac{mg\delta}{2}, \quad (1)$$

where: F_a, F_b are the maximum vertical force borne by the axle housing at this time; δ is dynamic load coefficient; G_1 is the maximum load of the vehicle at rest and full load, and is also the reaction force of the wheel given by the ground; m is total vehicle mass; g is acceleration of gravity.

With reference to the design parameters of the vehicle, we can get that the total mass m of the vehicle is 4.495 t (4495 kg); g is 9.8 m/s^2 ; δ generally takes 2.5.

After entering the data into the formula: $F_1 = 55063.75 \text{ N}$.

Finite element analysis of driving axle housing under maximum vertical force condition. The specific operation of boundary condition setting and load application: for the left half axle sleeve of axle housing, only the translational degrees of freedom in 3 directions are constrained; For the right end, the translational degrees of freedom are constrained except in the x-direction, but the rotational degrees of freedom on the X-axis are also constrained at both ends. At the same time, on both sides of the spring seat, apply a positive force along the Z axis, the magnitude of which is 55063.75 N. Then, an in-depth finite element analysis was carried out, and the corresponding Von Mises distribution and total deformation program were obtained, as shown in Fig. 5 and Fig. 6.

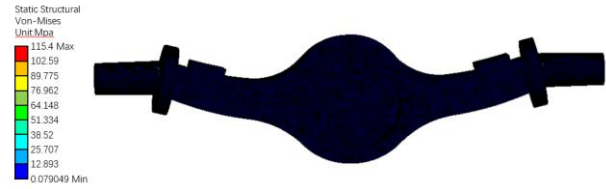


Fig. 5 Von Mises nephogram of axle housing under maximum vertical force condition

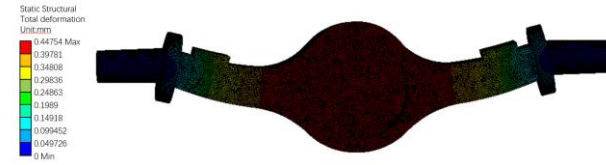


Fig. 6 Deformation cloud image of axle housing under maximum vertical force condition

3.2 Modal analysis of drive axle housing

Modal analysis is an effective means to investigate structural vibration and its dynamic characteristics, which is widely used in the field of engineering vibration. In addition, modal analysis not only helps us to accurately calculate the natural frequency of the structure but also helps us to determine the corresponding mode, which can truly show the vibration behavior of the structure. The generalized dynamical governing equations describe the theoretical basis of the dynamical characteristics.

$$[M][\ddot{x}] + c[\dot{x}] + [K][x] = [F], \quad (2)$$

where: $[M]$ is mass matrix; $[\ddot{x}]$ is node acceleration vector; c is damping matrix; $[\dot{x}]$ is node velocity vector; $[K]$ is stiffness matrix; $[x]$ is node displacement vector; $[F]$ is time varying external loads.

ANSYS sets the boundary conditions and imposes loads on the axle housing under normal working conditions, constraining the translational degrees of freedom in three directions and the rotational degrees of freedom in X direction for the bushings on both sides of the axle housing. Then, through in-depth finite element analysis, the first six vibration frequencies of the axle housing and the corresponding ground vibration mode data are obtained, and the vibration characteristics of the axle housing under different frequencies are directly reflected in Fig. 7 to Fig. 12.

In the normal operation of the vehicle, the road excitation is the key factor that leads to the failure of the axle and may cause resonance. According to the available data, the excitation frequency of the road surface is usually lower than 50 Hz. After in-depth finite element analysis, we successfully obtained the first 6-order natural frequencies and vibration modes of the drive axle housing under constrained modes. After detailed observation, it is found that the natural frequency of each order mode and its corresponding value are far more than the road excitation Hertz of 0~50 Hz, which ensures that the resonance will not occur. To ensure the pertinence, simplicity, and accuracy of the subsequent analysis, the first six vibration modes of the axle housing are specially proposed for analysis and display.

From Figs. 7-12 and Table 2, it can be seen that the natural frequency of the first-order mode is 133.81 Hz, with

longitudinal (Y-direction) bending dominating. The natural frequency of the second-order mode is 192.21 Hz, with vertical (Z-direction) bending being the main bending. When the frequency of the third-order mode increases to 324.55 Hz, it mainly bends in the longitudinal direction (Y direction). The natural frequency of the fourth mode is 411.08 Hz, and torsion around the Z-axis is predominant. The fifth mode frequency is 453.59 Hz, and torsion around the Y-axis is the main factor. Finally, the sixth mode exhibits a third-order torsional characteristic of the Y-axis with a frequency of 747.75 Hz.

The frequency and mode characteristics of the drive axle housing in the constraint mode order 1-6 are analyzed. In the third mode, the axle housing is mainly dominated by the longitudinal bending mode.

To sum up: the axle housing meets the national standard and the design is reasonable.

4. Lightweight Design of Drive Axle Housing

The study of lightweight automobiles refers to reducing the weight of automobile components while ensuring stable performance and optimal performance after optimization so that the vehicle can still be driven safely. The most common lightweight methods currently include changes in material properties, improvements in manufacturing processes, and changes in the overall or local structure. To achieve the goal of lightweight drive shaft, the proposed method is to optimize the design of the drive shaft using size optimization in structural optimization, with the optimization goal being to minimize the weight of the drive shaft.

4.1. Optimization method

In general, the conditions for optimizing the structure and generating the optimal solution are as follows. Objective function:

$$\min f(X). \quad (3)$$

Constraint condition:

$$g_j(X) \leq 0. \quad (4)$$

Plug in the Lagrange factor

$$L(X, \mu) = f(X) + \mu^T g = f(X) + \mu_j g_j. \quad (5)$$

When finding the minimum value, the Lagrange equation needs to satisfy the conditions:

$$\begin{cases} \nabla_x L(X) = \nabla_x f(X) + \sum \mu_j \nabla_x g_j = 0, \\ \nabla_\mu L(\mu) = g = 0, \\ \mu_j^T g_j = 0, \\ \mu_j = 0. \end{cases} \quad (6)$$

The strength is reflected in: under the action of force, the maximum Von Mises of the axle housing cannot exceed the yield strength of the material; The stiffness is reflected in: the maximum deformation of the axle housing does not exceed 2.409 mm.

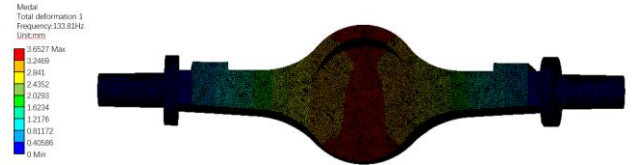


Fig. 7 First-order constrained modal analysis

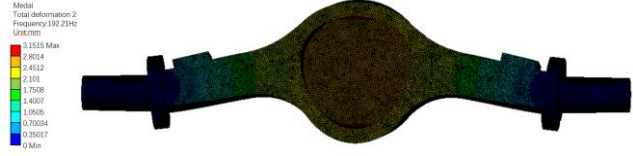


Fig. 8 Second-order constrained modal analysis

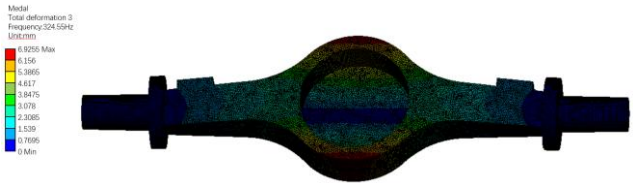


Fig. 9 Third-order constrained modal analysis

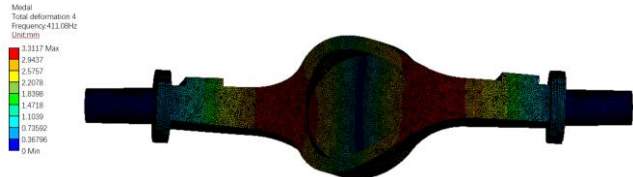


Fig. 10 Fourth-order constrained modal analysis

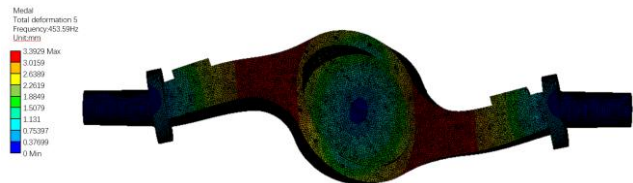


Fig. 11 Fifth-order constrained mode analysis

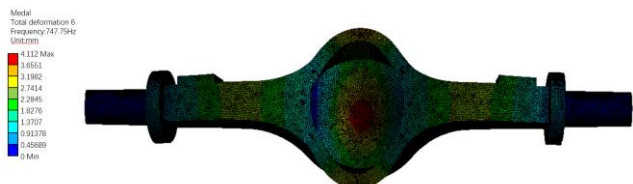


Fig. 12 Sixth-order constrained modal analysis

Objective function:

$$M = \min f(x_1, x_2, x_3). \quad (7)$$

Constraint conditions:

$$\delta \leq 310 \text{ MPa}, \quad (8)$$

$$Y \leq 2.409 \text{ mm}. \quad (9)$$

Design variables:

$$x_1 \leq 25 \text{ mm}, \quad (10)$$

Modal analysis of drive axle housing

Modal analysis	Frequency	Mode of vibration
First-order mode	133.81 Hz	Longitudinal (Y direction) bending mode
Second-order mode	192.21 Hz	Vertical (Z direction) bending mode
Third-order mode	324.55 Hz	Longitudinal (Y direction) bending mode
Fourth-order mode	411.08 Hz	Torsion mode about Z axis
Fifth-order mode	453.59 Hz	Torsion mode about Y axis
Sixth-order mode	747.75 Hz	Y-axis third order torsional mode

$$x_2 \leq 20 \text{ mm}, \quad (11)$$

$$x_3 \leq 25 \text{ mm}. \quad (12)$$

Here: M is the quality of the drive axle housing; δ is the stress of the front shell of the casing and the bridge housing of the plate spring seat; Y is the maximum deformation of the axle housing; x_1 is the axle housing wall thickness; x_2 is the thickness of the spring seat and x_3 is the thickness of the front axle housing.

The initial number of sample points is set to 40 and modified through sampling calculation. Finally, 40 sample points of axle housing size optimization design variables were obtained, and only the first 20 points were intercepted, as shown in Table 3.

To verify the accuracy of the model, 3 samples are randomly selected for analysis and calculation, and the system will automatically recommend 3 best candidate points for selection. The candidate points are shown in Table 4.

According to the experimental goal, the third set of proxy models was selected, and their size data was inputted into the upstream structural analysis, and then the data was updated for subsequent analysis.

4.2. Structural performance comparison

4.2.1. Strength property comparison

When comparing strength properties, it is only necessary to consider the conditions under the maximum vertical force. As can be seen from Fig. 13 and Fig. 14, the axle housing stress changes from 115.4 MPa to 115.3 MPa, reducing by 0.1 MPa, as shown in Table 5, indicating that the distribution of Von Mises is more and more average and less than the allowable stress of 206.67 MPa, so the axle housing still meets the design requirements at this time.

4.2.2. Stiffness performance comparison

By comparing the total deformation cloud map of the lightweight front and rear axle housing under the maximum vertical force condition, it can be seen from Fig. 15 and Fig. 16 that the deformation of the axle housing is increased from 0.44754 mm to 0.49929 mm, with a variation of 0.05175 mm as shown in Table 6. However, the wheel

Table 3

Sample points

Serial number	Axle housing thickness	Spring seat height	Spring seat width	Total deformation, mm	Von Mises, MPa
1	25	25	20	0.48381	95.784
2	26.287	27.975	22.755	0.46282	92.815
3	27.718	22.114	17.696	0.46124	81.911
4	21.9	23.053	17.989	0.53397	102.81
5	21.785	28.645	16.629	0.51858	91.751
6	21.798	21.62	23.657	0.54005	98.415
7	22.071	27.145	22.563	0.5176	95.248
8	27.258	26.899	17.481	0.45572	86.394
9	27.041	22.044	21.516	0.46781	96.15
10	24.012	25.461	16.284	0.49595	97.344
11	26.598	29.978	19.241	0.45606	84.912
12	24.516	20.184	15.185	0.50432	100.08
13	24.934	24.409	24.985	0.50432	100.08
14	20.405	20.302	15.339	0.573	103.16
15	20.218	20.081	20.24	0.57702	104.89
16	25.601	29.732	15.143	0.46748	80.968
17	25.261	20.06	24.998	0.49343	92.1
18	29.63	24.404	15.073	0.44045	83.058
19	24.247	20.031	19.537	0.48381	95.784
20	20.134	29.551	20.096	0.54288	96.447

Table 4

Selects three agent model points

Serial number	Name	Candidate point 1	Candidate point 2	Candidate point 3
1	Axle housing thickness	23.732	23.092	20.532
2	Spring seat height	29.772	29.758	29.728
3	Spring seat width	16.79	15.582	18.253
4	Total deformation, mm	0.48577	0.49536	0.53308
5	Von Mises, MPa	87.421	88.659	88.149
6	Quality, kg	158.39	155.85	148.08

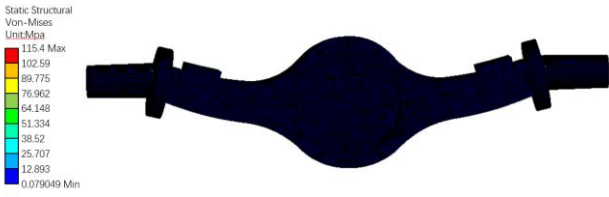


Fig. 13 Stress distribution diagram of axle housing before optimization

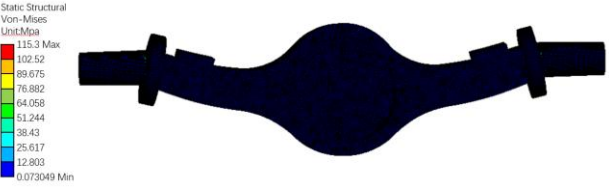


Fig. 14 Stress distribution diagram of axle housing after optimization

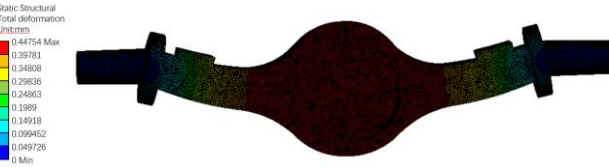


Fig. 15 Total deformation cloud image of axle housing before optimization

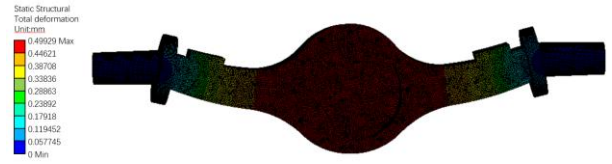


Fig. 16 Total deformation cloud image of axle housing after optimization

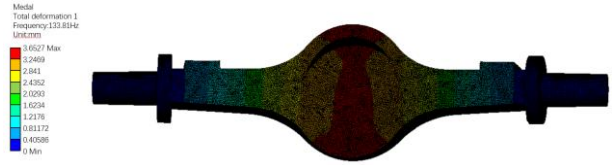


Fig. 17 First-order modal of axle housing before lightweighting

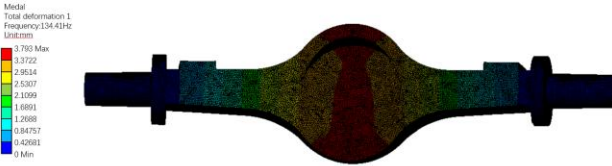


Fig. 18 First-order modal of axle housing after lightweighting

Table 5

Maximum stress value and comparison of axle housing before and after lightweight

Maximum vertical force condition	Before optimization	Post-optimization	Variation
Maximum Von Mises value	115.4 MPa	115.3 MPa	-0.1 MPa

Table 6

Maximum deformation value and comparison of axle housing before and after lightweight

Maximum vertical force condition	Before optimization	Post-optimization	Variation
Maximum deformation value	0.44754 mm	0.49929 mm	0.05175 mm

Table 7

Constraint modal analysis table before and after lightweight

The number of modal orders	Order 1	Order 2	Order 3	Order 4	Order 5	Order 6
Pre-optimization frequency	133.81 Hz	192.21 Hz	324.55 Hz	411.08 Hz	453.59 Hz	747.75 Hz
Optimized frequency	134.41 Hz	193.15 Hz	328.64 Hz	421.78 Hz	456.21 Hz	760.82 Hz
Frequency variation	0.6 Hz	0.94 Hz	4.09 Hz	10.7 Hz	2.62 Hz	13.07 Hz
Mode of vibration	Longitudinal bending	Vertical bending	Longitudinal bending	Twist around the Z axis	Twist around the Y axis	Y-axis third order torsion

base per meter is 0.33 mm/m, and the maximum allowable deformation is not more than 1.5 mm/m, so the stiffness of the axle housing also meets the working requirements.4.2.3. Modal frequency comparison

The frequency and mode characteristics of the constrained modes 1-6 after optimization of the drive axle housing are analyzed as shown in Table 7. In the first mode, the axle housing reaches the maximum shape variable with a value of 3.793 mm, which is mainly dominated by the Y-axis distortion mode. After detailed observation, it is found that the natural frequency value of each order mode and its corresponding value are far more than the road excitation

Hertz of 0~50 Hz, it can be concluded that the structure of the drive axle housing meets the requirements and the performance is good. The obtained first-order natural frequency and mode are shown in Fig. 17 and Fig. 18.

5. Conclusions

The system lightweight optimization design of the axle housing model was carried out, and the accuracy and reliability of the finite element analysis data were verified by analyzing and comparing the strength, stiffness, natural frequency, and vibration mode of the optimized model under working conditions. The thickness of each part of the

axle housing was optimized and adjusted, so that the total weight of the axle housing was reduced from 169.4 kg to 156.83 kg, and the weight was reduced by 7.42%.

The specific performance is: for the non-load-bearing parts of the axle housing, the size optimization method is used. With the goal of minimizing mass in ANSYS, the optimization variables are set as axle housing wall thickness, leaf spring seat and front axle housing thickness, and the constraint conditions are set as two kinds of performance of axle housing.

1. Through iterative calculation, the paper optimized and adjusted the thickness of each part of the axle housing, reducing the total weight of the axle housing from 169.4 kg to 156.83 kg, and the weight reduction reached 7.42%. The wall thickness of the axle housing increased from 25 mm to 29.782 mm, the thickness of the plate spring seat decreased from 20 mm to 18.253 mm, and the thickness of the front axle housing decreased from 25 mm to 20.532 mm.

2. Compared with before optimization, the stress distribution of the optimized drive axle housing under the maximum vertical force condition is more uniform, its stress is reduced by 0.1 MPa, and its shape variable is also increased by 0.05175 mm. Through comparative analysis, the optimized axle housing still conforms to the national standard and has good performance.

3. Compared with the constrained modes before and after optimization, the first-order natural frequency of the optimized axle housing is increased by 0.6 Hz. In the fifth mode, the natural frequency changes the most, and its value is 328.64 Hz. In the constrained mode, the deformation resistance of the axle housing is enhanced with the increase of the shape variable. In addition, the first six natural frequencies are still higher than the road excitation frequency, which means that the axle housing will not resonate in actual use and has good performance.

According to the above experimental results, the drive axle housing used in the experiment meets the requirements of national standards in terms of strength and stiffness, and there is still a potential for lightweight. In the design process, the thickness of the front axle housing, the thickness of the leaf spring seat, and the wall thickness of the axle housing are taken as parameter variables, the constraint conditions are set as stiffness and strength, and the core optimization objective is to reduce the quality of the axle housing. In summary, the lightweight axle housing not only successfully achieved the weight reduction goal, but also maintained good static and dynamic performance.

Acknowledgments

This project comes from the research and development and application demonstration of electric caterpillar multi-functional farm management machine. This work was financially supported by Yibin Science and Technology Program (grant No.2022NY00901).

References

1. **Nicoletti, L.; Romano, A.; Knig, A.; Khler, P.; Lienkamp, M.** 2021. An estimation of the lightweight potential of battery electric vehicles, *Energies* 14(15): 4655. <https://doi.org/10.3390/en14154655>.
2. **Topaç, M. M.; Karaca, M.; Aksoy, B.; Deryal, U.; Bilal, L.** 2020. Lightweight Design of a Rear Axle Connection Bracket for a Heavy Commercial Vehicle by Using Topology Optimisation: A Case Study, *Mechanika* 26(1): 64-72. <https://doi.org/10.5755/j01.mech.26.1.23141>
3. **Prabhakar, M.; Prasad, A. K.; Paswan, M. K.** 2020. Realistic Correlation of Damage Estimate in Axle Housing of Commercial Vehicles Using Road Load Data with Bench Testing Results and Failure Analysis to Overcome Hot Forming Losses, *SAE International Journal of Commercial Vehicles* 14(1): 3-21. <https://doi.org/10.4271/02-14-01-0001>.
4. **Zhao, F.** 2021. Finite-element analysis on lightweight material of drive axle housing, *Revue des Composites et des Materiaux Avances – Journal of Composite and Advanced Materials* 31(1): 41-49. <https://doi.org/10.18280/rcma.310106>.
5. **Liu, B. L.; Xie, L. Y.; Zhang, N.; Luo, Y. J.** 2018. Finite element modeling of punching drive axle housing parameterization based on insight, *Journal of Northeastern University: Natural Science Edition* 39(3): 373-377. <https://doi.org/10.12068/j.issn.1005-3026.2018.03.014>.
6. **Chen, Y.; Liu, X.; Shan, Y.; He, T.** 2020. Lightweight design of drive axle housing based on reliability, *International Journal of Vehicle Performance* 6(3): 294-309. <https://doi.org/10.1504/IJVP.2020.109185>.
7. **Zheng, B.; Fu, S.; Lei, J.** 2022. Topology Optimization and Multiobjective Optimization for Drive Axle Housing of a Rear Axle Drive Truck, *Materials* 15(15): 5268. <https://doi.org/10.3390/ma15155268>.
8. **Mi, C.; Li, Y.; Zhang, C.; Zhang, D.; Liu, X.; Hu, X.; Zhang, D.** 2023. An Energy-Based Anti-Fatigue Optimization Design Method of Welded Rear Axle Housing in a Mining Dump Truck, *Mechanika* 29(4): 317-323. <https://doi.org/10.5755/j02.mech.32371>.
9. **Zou, Z.; Xu, F.; Wang, D.; Fang, T.; Jiang, Z.** 2024. Database-driven lightweight design for axle housing of heavy-duty truck, *Proceedings of the Institution of Mechanical Engineers, Part D: Journal of Automobile Engineering*: 09544070241233776. <https://doi.org/10.1177/09544070241233776>.
10. **Agarwal, A.; Mthembu, L.** 2022. Weight optimization of heavy-duty truck chassis by optimal space fill design using light weight Graphite Al GA 7-230 MMC, *Materials Today: Proceedings* 52(3): 1278-1287. <https://doi.org/10.1016/j.matpr.2021.11.053>.
11. **Gür, Y.; Cen, G.** 2024. Comparison of finite element analysis results with strain gauge measurements of a front axle housing, *Mechanical Sciences* 15(1): 257-268. <https://doi.org/10.5194/ms-15-257-2024>.
12. **Talay, E.; Özkan, C.; Gürtaş, E.** 2021. Designing lightweight diesel engine alternator support bracket with topology optimization methodology, *Structural and Multidisciplinary Optimization* 63: 2509-2529. <https://doi.org/10.1007/s00158-020-02812-z>.
13. **Prabhakar, M.; Prasad, A. K.; Paswan, M. K.** 2020. Influence of loading sequence and residual stresses affecting the fatigue life of axle housing and crack path analysis using local approaches, *Engineering Failure Analysis* 116: 104753. <https://doi.org/10.1016/j.engfailanal.2020.104753>.
14. **Topaç, M. M.; Günal, H.; Kuralay, N. S.** 2009. Fatigue failure prediction of a rear axle housing prototype

- by using finite element analysis, *Engineering Failure Analysis* 16(5): 1474-1482.
<https://doi.org/10.1016/j.engfailanal.2008.09.016>.
15. **Kurniawan, A.; Andoko.** 2019. Stress and Crack Simulation on Axle Housing Mitsubishi L300 Pickup Car using Finite Element Method. In *IOP Conference Series: Materials Science and Engineering* 494(1): 012107.
<https://doi.org/10.1088/1757-899X/494/1/012107>.
 16. **Ognevskii, V. A.; Orlovskii, A. G.; Ostrovkii, G. A.; Ryskind, A. M.; Trofimov, O. F.; Shklyarov, I. N.** 1977. Increase in the strength of rear axles due to electrothermal treatment, *Metal Science and Heat Treatment* 19(9): 774-777.
<https://doi.org/10.1007/BF00670275>.
 17. **Fu, J. S.; Wang, J.; Wang, J. F.** 2010. Finite Element Analysis and Structure Optimization on Light-Duty Truck Driving Axle Housing, *Applied Mechanics and Materials* 37-38: 482-485.
<https://doi.org/10.4028/www.scientific.net/AMM.37-38.482>.
 18. **Xu, J. L.; He, Q.; Zhu, D. J.** 2017. Lightweight Research on Aluminum Alloy Material of Rear Axle Differential, *Key Engineering Materials* 723: 294-298.
<https://doi.org/10.4028/www.scientific.net/KEM.723.294>.
 19. **Rishi, J. P.; Srinivas, T. R.; Ramachandra, C. G.** 2018. A Study on Lean Manufacturing Practice Carried Out for Axle Housing Plant, In *MATEC Web of Conferences* 144: 05005.
<https://doi.org/10.1051/mateconf/201814405005>.
 20. **Kumar, G. S.; Kumaraswamidhas, L. A.** 2021. Design optimization focused on failures during developmental testing of the fabricated rear-axle housing, *Engineering Failure Analysis* 120: 104999.
<https://doi.org/10.1016/j.engfailanal.2020.104999>.
 21. **Cosme, C.; Ghasemi, A.; Gandevia, J.** 1999. Application of Computer Aided Engineering in the Design of Heavy-Duty Truck Frames, *SAE Technical Paper* 1999-01-3760.
<https://doi.org/10.4271/1999-01-3760>.
 22. **Pirmohammad, S.; Esmaeili-Marzdashti, S.** 2019. Multi-objective crashworthiness optimization of square and octagonal bitubal structures including different hole shapes, *Thin-Walled Structures* 139: 126-138.
<https://doi.org/10.1016/j.tws.2019.03.004>.

T. Zhang, H.J. Wang, Q. Yang

RESEARCH ON THE LIGHTWEIGHT DRIVE AXLE HOUSING OF ELECTRIC FARM MANAGEMENT MACHINE

S u m m a r y

The paper shows that the drive axle housing of the electric farm management machine not only has the role of carrying and transmitting power, but also plays a supporting role for the main reducer, brake and other components, which needs to meet the requirements of stiffness and strength. Three-dimensional modeling and finite element analysis are used to design the joint, and a reasonable three-dimensional modeling of the drive axle housing is carried out. Aiming at the structural quality of the axle housing, the finite element analysis method is used to reduce the quality of the axle housing. Firstly, the force analysis is carried out according to the maximum vertical force condition of the drive axle housing. Secondly, the static and dynamic characteristics of the axle housing structure are analyzed. Then, with the parameters that have great influence on the quality as the design variables, the quality of the axle housing as the optimization objective, and the maximum static stress and maximum deformation as the constraint conditions, the Latin hypercube experimental design method and genetic optimization algorithm are used to carry out the lightweight design of the axle housing. Finally, through the optimization scheme, the total weight of the axle housing using structural steel is reduced from 169.4 kg to 156.83 kg, achieving a weight reduction effect of 7.42%, and realizing the lightweight of the axle housing.

Keywords: Axle housing; lightweight optimization; mechanical stiffness; mechanical strength.

Received June 25, 2024

Accepted December 16, 2024



This article is an Open Access article distributed under the terms and conditions of the Creative Commons Attribution 4.0 (CC BY 4.0) License (<http://creativecommons.org/licenses/by/4.0/>).